IEEE Access
Multidisciplinary | Rapid Review | Open Access Journal

Received February 21, 2020, accepted March 13, 2020, date of publication March 19, 2020, date of current version March 31, 2020.

Digital Object Identifier 10.1109/ACCESS.2020.2982048

Multimodal Recognition System Based on High-Resolution Palmprints

INASS SHAHADHA HUSSEIN[1,2], SHAMSUL BIN SAHIBUDDIN[1], MD JAN NORDIN[3], (Member, IEEE), AND NILAM NUR BINTI AMIR SJARIF[1]

[1]Faculty Razak of Technology and Informatics, Universiti Teknologi Malaysia (UTM), Kuala Lumpur 54100, Malaysia
[2]Baquba Technical Institute, Middle Technical University, Baquba 32001, Iraq
[3]Faculty of Information Science and Technology, Universiti Kebangsaan Malaysia (UKM), Bangi 43600, Malaysia

Corresponding author: Inass Shahadha Hussein (inasshussin@yahoo.com)

This work was supported in part by the Universiti Teknologi Malaysia (UTM) and in part by the Universiti Kebangsaan Malaysia (UKM) under Grant DIP-2016-018.

ABSTRACT High-resolution palmprint recognition is a challenging problem due to deficiencies in images, such as poor quality, skin distortion, and unallocated images. Considering the importance of high-resolution palmprints in forensic applications, this study proposes a novel multimodal palmprint scheme that combines the left and right palmprints using feature-level fusion by exploiting the similarity between the left and right palmprints using high-resolution images. The proposed system accepts as input palmprints that were captured at 500 ppi, which is the standard in forensic applications. The system is implemented by employing a statistical gray-level co-occurrence matrix (GLCM) as the texture feature extraction algorithm. Then, the features are ranked based on their probability distribution functions (PDFs) to select the most significant features. Finally, an enhanced probabilistic neural network (PNN) is used to estimate the recognition system. The benchmark THUPALMLAB database is used to conduct experiments, the results of which demonstrate that the proposed method can yield satisfactory results.

INDEX TERMS GLCM, high-resolution palmprint, multimodal, PNN, ranking features.

I. INTRODUCTION

A palmprint is a well-accepted biometric that is simple to capture and difficult to forge. The friction ridges and creases in palmprints are unique for each individual and remain fixed throughout life [1]. Palmprint biometrics have been widely used for both civil and forensic applications [2]–[5]. A palmprint recognition system can be either unimodal or multimodal. A unimodal system is based on a single trait. This model is widely used due to its simplicity; however, it suffers from several limitations, such as noise in the sensor when the data are collected, intraclass variations, non-universality, and spoof attacks [6]. To overcome the limitations of the unimodal system and to increase the security, a multimodal system was suggested. Multimodal systems use two or more traits to obtain the desired results [7]. Several researchers proposed palmprint multimodal systems that combine traits [8]–[13]. However, these studies were limited to low-resolution palmprints. Although these studies yielded satisfactory results, they suffered from various problems, such as a lack of databases that contain two distinct traits that belong to the same person, long execution times, and differences in terms of the feature types and dimensions [14].

To overcome these problems, a multimodal system that is based on the left and right palmprints was proposed, as the prints on a person's left and right palms are similar [15], [16]. References [15] and [16] described the following advantage of combining the left and right palmprints: the palmprint images of the right and left hands of each user are similar. These similarities were employed to improve the performance and increase the accuracy rate of palmprint identification. However, research on this model remains limited, and several aspects require improvement.

In addition, based on the resolution, palmprint images can be classified as either low-resolution or high-resolution images [17]. The low-resolution recognition methods can be categorized into three types: principle line, subspace learning, and texture-based methods. Among these three types of methods, the texture-based method has high recognition accuracy [5].

The associate editor coordinating the review of this manuscript and approving it for publication was Inês Domingues.

In contrast, most high-resolution palmprint recognition methods were adopted from the fingerprint recognition system [18], [19]. The main feature in high-resolution palmprint images is based on texture, as these images contain ridges and minutiae points and share a similar texture pattern with fingerprint images [20]. According to [17], there are three major feature extraction methods for high-resolution palmprints: local ridge direction (LRD), minutia points, and principle line methods. However, the palmprint images are typically of poor quality since crime scene prints are not left intentionally; thus, an ambient environment can render the prints distorted. Furthermore, most of the feature details cannot be obtained; thus, feature extraction is difficult. In this study, we combine the advantages of the palmprint multimodal system and the importance of high-resolution images to develop a high-resolution palmprint multimodal scheme by employing the following:

- a high level of multimodal security;
- the similarity between the right and left palmprints; and
- the extraction of multiple texture features.

Toward this objective, we propose a scheme that includes several steps. Initially, multiple statistical features are extracted based on the GLCM algorithm from high-resolution palmprints from both left and right hands. Then, the features are fused using the feature-level fusion approach. Next, a new filter ranking method that is based on the statistical probability distribution function (PDF) is used to select high-ranking features. Finally, these features are evaluated via PNN in the recognition phase. The PDF has been successfully applied to classification problems such as Alzheimer's disease detection and face recognition [21], [22]. Moreover, the robustness and efficacy of implementing PNNs have resulted in a variety of applications in classification problems in several research areas, such as computer science, electrical engineering, civil engineering, and biomedical engineering [23], [24].

The remainder of the paper is organized as follows: Section II reviews the literature. Section III describes the proposed method, and Section IV presents the experimental results. Finally, the conclusions are presented in Section V.

II. LITERATURE REVIEW

This section compiles the most prominent studies that are based on high-resolution palmprint images. The first known use of palmprint biometrics in a criminal case occurred in a British court in 1930, while the first palmprint identification system was available in the 1990s [25]. Many researchers have considered degraded partial palmprint images in their studies. The partial palmprint rotation-invariant and degraded recognition (PP-RIDER) technique was introduced by Singh *et al.* [26]. This technique corrected the arbitrary rotation of a partial palmprint for comparison with a full palmprint image in the database. The PP-RIDER technique is based on the Fourier transform (FT) of the input image and combines the FT to amend the random rotation technique for the partial image against the full image and employs the modified phase-only correlation (MPOC) for the matching phase. In addition, Singh *et al.* [27] improved the PP-RIDER technique by using a different interior lobe size. Through the addition of the degradation case, Gaussian noise, and motion blur to the partial palmprint, they conducted three experiments with interior lobe sizes of 61×61 and 101×101 by using the THUPALMLAB modified database.

Carreira *et al.* [1] extended this approach using high-resolution palmprints that matched the partial or degraded palmprints. They presented a new technique for motion blur detection and compensation that is based on the work of Brusius *et al.* [28] and uses an adaptive filter to handle Gaussian noise and a median filter to deal with salt-and-pepper noise. This study also proposed the segmentation of the palmprint area and used the scale-invariant feature transform (SIFT) algorithm for feature extraction to detect key points. The matching relied on the SIFT keypoint descriptor comparison. This approach is called partial palmprint–keypoint matching degraded recognition (PP-KMDR).

Then, Carreira *et al.* [29] combined the methods that were proposed in two earlier studies [1], [26] by selecting between two palmprint matching approaches, and they obtained a better result than the results of the two individual methods. The PP-KMDR and PP-RIDER techniques were used after preprocessing the image. The decision was based on the results of these algorithms.

Wang *et al.* introduced approaches that are based on high-resolution palmprints. In 2012, they [30] introduced a latent-to-full palmprint biometric system that is based on triangulation and logistic regression learning for score computation. This study was evaluated on a forensic database that included 22 latent palmprints from real cases and 8680 full palmprints from criminal investigations.

In 2013, Wang *et al.* [31] further developed an automatic region segmentation method, which could segment an image into three regions, namely, interdigital, thenar, and hypothenar regions, by applying a Canny edge detector to a full palmprint image, detecting the first data point by the convex hull, and estimating based on the position and direction of the first data point. Finally, the regions were segmented based on these points. The accuracy of this approach was compared with that of the manual segmentation method on the THUPALMLAB database.

In the same year, Wang *et al.* [32] used these three regions to propose a matching strategy based on regional fusion, which includes two stages: first, to calculate the region-to-region palmprint comparison score, a commercial SDK (Software Development Kit), namely, Mega Matcher 4.0, is used for feature extraction and matching. Second, regional fusion at the score level is implemented by applying the FoCal Toolkit to the region-to-region matching score that was obtained in the first stage. Then, they compare the result with the full palmprint score by using Mega Matcher 4.0. This system was evaluated on the last 50 subjects ($50 \times 2 \times 8$) from the THUPALMLAB database.

TABLE 1. Previous studies on high-resolution palmprints.

Reference	Recognition algorithm	Features	Parameter	Palmprint type	Database/Size
[25]	Minutiae matching	Minutia code	Rank-1 recognition rates = 78.7%	Latent	Latent/100
			Rank-1 recognition rates = 69%	Partial	Live scan/150
[34]	MOPOC	2D discrete Fourier transform	EER= 0.4%.	Partial	Generated/800
[35]	Weighted sum, Neyman-Pearson, or SVM	Minutiae, density, orientation, and principle lines	Rank-1 recognition rates= 91.7% EER= 4.8%	Full	THUPALMP/14,576
[30]	Logistic regression learning	Minutiae	Rank-1 recognition rates =69%	Latent	latent palmprints/22 full palmprint/8680
[27]	MPOC	Fourier–Mellin transform (FMT)	EER= 27.11%	Partial	Modified THUPALMP/8
			EER= 21. 525%	Partial	PV-TESTPARTIAL/4
			EER= 19.54%	Full	
[32]	Mega Matcher and FoCal Toolkit	Major creaser	EER=0.25%	Partial	THUPALMLAB/ subset from last 50 subjects (50×2×8)
			EER = 1%	Full	
[33] Manual regions,%	Sum rule and logistic regression	SMC	ERR = 11.11% = 17.5% = 5.46%	Partial: Interdigital, Thenar, Hypothenar	THUPALMLAB/ subset from last 50 subjects (50×2×8).
			EER= 14.2%	Full	
[33] Automatic regions,%	Sum rule and logistic regression	SMC	EER = 8.95% = 16.43% = 4.08%	Partial: Interdigital, Thenar, Hypothenar	THUPALMLAB/ subset from last 50 subjects (50×2×8)
			EER= 11.64%	Full	
[1]	SIFT	SIFT descriptor	ERR= 22.55% Rank-1 recognition rates =93.75%	Partial	THUPALMLAB/ (160×8×7), (10×8)
[36]	Global minutiae matching	Minutiae location, direction, and transformation	ERR = 0.002% Rank-1 recognition rates =100%	Partial: 4 half-palmprints	Private/200
			ERR = 0.88% Rank-1 recognition rates =98.73%	4 quarter-palmprints	
			ERR= 0%	Full	
			Rank-1 recognition rates =100%		

Then, in 2014, Wang *et al.* [33] extended their previous work by applying the spectral minutiae representation (SMC), which was used in minutiae-based fingerprint recognition, to region-to-region palmprint comparison (Interdigital, Thenar, and Hypothenar). Two experiments were conducted: first, a region-to-region comparison was made; then, the three regions were fused, and the results were obtained at the score level by using two fusion methods, namely, the sum rule and logistic regression. These regions were obtained manually and automatically by using the last 50 subjects ($50 \times 2 \times 8$) in the THUPALMLAB database.

According to the literature review, no study has been conducted on multimodal palmprints from high-resolution images.

Table 1 summarize the previous studies on high-resolution unimodal palmprints.

III. PROPOSED METHOD

In this section, the proposed multimodal palmprint scheme will be introduced in more detail. The proposed scheme consists of five steps, which include preprocessing, texture extraction, feature-level fusion, and recognition. In addition, the feature selection step will be a crucial step during feature fusion. Figure 1 depicts a general overview of the proposed scheme.

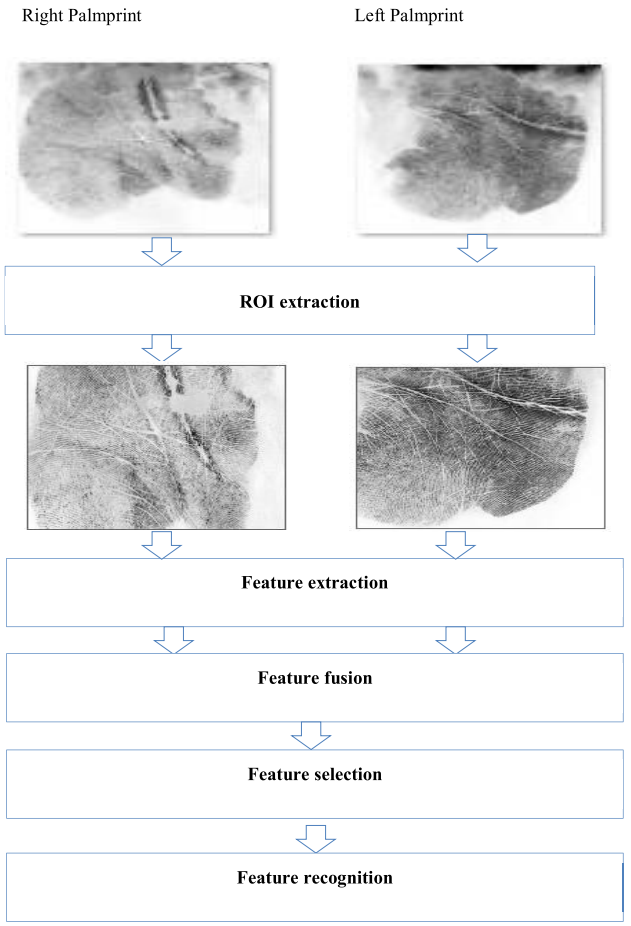

FIGURE 1. General overview of the proposed scheme.

A. PREPROCESSING

Preprocessing techniques are typically used to increase the quality of the image domain. Preprocessing includes noise removal and region of interest (ROI) extraction. The problems that are encountered with high-resolution images are caused mainly by variation in the location and distortion of the skin images. Therefore, it is difficult to extract ROIs. However, we adopted the ROI method that was reported in [37], which includes two phases, namely, the binarization phase and the ROI extraction phase. The binarization phase is comprised of three steps: first, noise removal using a median filter; second, 2D palmprint image histogram calculation; and third, binarization of the palmprint image by calculating the 2D histogram entropy and selecting the maximum entropy as a threshold value. The binary palmprint image that is obtained from the previous step is passed as input to the ROI extraction phase, which is conducted in two steps, namely, application of the dilation and ROI construction. The following steps summarize the complete approach: noise removal by using a median filter; binarization of the palmprint image by using the maximum entropy as an adaptive threshold; dilation of the binary image; ROI extraction from the dilated image; and conversion to gray level.

The findings of this work strongly demonstrate that the proposed method can extract the palm's ROIs consistently. These ROIs are used in the recognition system instead of the whole palmprint and, hence, facilitate the improvement of the performance of the traditional palmprint system. Figure 2 shows a palmprint and the ROI.

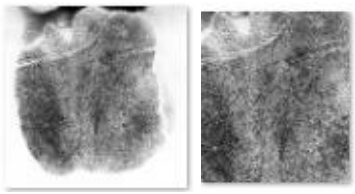

FIGURE 2. a. Palmprint b. ROI.

B. TEXTURE EXTRACTION

Most high-resolution studies used SMC as the minutiae representation, which is used in minutiae-based fingerprint recognition for palmprint comparison. However, the performance of SMC for full-to-full palmprint comparison is not satisfactory compared with either its performance in fingerprint matching or with the performances of the state-of-the-art methods in high-resolution palmprint recognition. This is partly because of the large size of palmprints compared with fingerprints. A high-resolution palmprint differs from a fingerprint as it has rich types of features in addition to minutiae, such as principal lines (major creases), minor creases, and texture. The use of texture features is a promising strategy, as the texture is an accurate feature for both low-resolution and high-resolution palmprints [17].

The texture can be defined as the basic element for perception in human vision. It is a set of calculated measurements in image processing. A statistical approach regards an image texture as a quantitative measure of the organization of intensities in an image. In addition to analyzing the spatial distribution of the gray values, the local features at each point in the image are calculated, which form a set of local statistical distribution features [38].

In this study, we adopted the statistical GLCM algorithm for texture extraction, which is a robust and effective technique for classification [39]. The GLCM algorithm transforms the palmprint images into a new matrix (0-255) that is based on the distribution of occurrences of intensity in the image by estimating image properties that are related to the second-order statistic [38], [39]. Although the ROIs

will differ in terms of size, the GLCM algorithm will transform the palmprint images into co-occurrence matrices of dimension (0-255). Hence, ROIs of various sizes will result in co-occurrence matrices of the same size. Mathematically, a GLCM is a square matrix of size $N \times N$; the gray-level image is divided into N intensity levels, which determine the size of the GLCM; each position(i, j) for an element of the matrix represents the frequency of co-occurrence of two pixels (reference pixel and neighbor) with intensities i and j, which correspond to a specified distance and direction. The frequency is denoted by $P(i, j, d, \theta)$, which is expressed as follows:

$$p(i,j,d,\theta) = \{(x,y), (x+D_x, y+D_y) | f(x,y) = i, f(x+D_x, y+D_y) = j\} \quad (1)$$

where x *and* y are the spatial positions on $N \times N$, and D_x and D_y are the offsets, which determine the direction of the distance d between the reference pixel and its neighbor, respectively, which render the matrix sensitive to rotation. Based on θ, each pixel has eight neighbors (0°, 45°, 90°, 135°, 180°, 225°, 270°, and 315°). GLCM is symmetric, namely, GLCM at $\theta = 0°$ is similar to GLCM at $\theta = 180°$ and so on, where $GLCM_{i,j} = GLCM_{j,i}$. Thus, the offset will be affected by the rotation that corresponds to angles 0°, 45°, 90°, and 135°, and these angles correspond to four directions (p horizontal, p right direction, p vertical, and p left direction). By regarding the distance between the reference pixel and its neighbor (d) as equal to 1, 14 texture features are extracted from each co-occurrence matrix according to the directions 0°, 45°, 90°, and 135°. These feature vectors are called Haralick feature vectors [40]. In this study, we used 13 features (we ignored the 14th feature due to its complicated calculation) from four directions (angular second moment, contrast, correlation, sum of square or variance, inverse difference, sum average, sum variance, sum entropy, entropy, difference variance, difference entropy, first information measure, and second information measure). These features are fused in the subsequent step.

C. FEATURE FUSION

In this step, two or more trait features are fused into a single feature vector. The feature level that offers better identification than other levels utilizes a feature set through various vector sequence features in the large vector form, which contains more information on feature traits [14], [41]–[43]. The concatenation rule is used to combine feature vectors [44]. $\boldsymbol{F\ fused}$ is calculated as $\boldsymbol{F\ fused} = \boldsymbol{fK} \times (\boldsymbol{m} + \boldsymbol{n})$. The first feature set $= \boldsymbol{f1k} \times \boldsymbol{m}$, and the second feature set $= \boldsymbol{f2k} \times \boldsymbol{n}$, where $\boldsymbol{m}$ *and* $\boldsymbol{n}$ are the feature dimensions and, $\boldsymbol{k} = \boldsymbol{1}$. The output of the feature extraction and feature fusion steps is a feature matrix database, which is built as presented by Algorithm 1 and illustrated in Figure 3.

To reduce the dimension of the feature vectors and to select the most effective feature, the features are fed into the feature selection calculation.

Algorithm 1 Extraction and Fusion of Features

Input NC = number of palmprints, NS = number of samples per palmprint

Step 1: Apply GLCM

For k = 1, k ≤ NC, k++

For f = 1, f ≤ NS, f++

- Input (left ROI palmprint (k, f), right ROI palmprint (k, f);
- Set d = 1, θ = (0°, 45°, 90°, and 135°)
- Apply GLCM[] (d, θ);

Step 2: Apply Haralick feature functions;

Step 3: Apply standardization function;

Step 4: Apply concatenation rule;

- Save to database;
- Repeat;
- Output: matrix [i, j]; where i = number of features, j = NS × NC

Step 4: Go to selection step

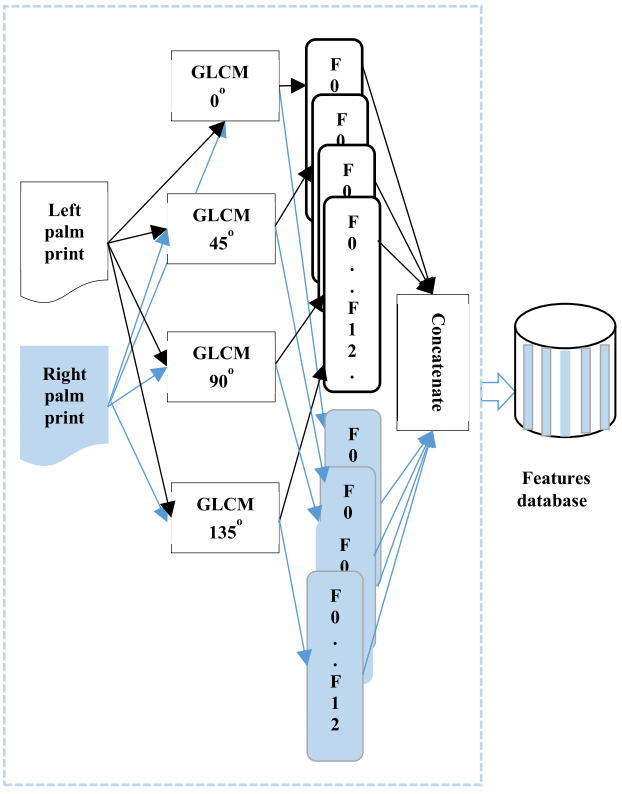

FIGURE 3. Feature extraction and fusion model.

D. FEATURE SELECTION

Feature selection is an additional step that is used to reduce the dimension of the feature vector. This study employed the ranking feature method for feature selection. The ranking feature is a simple filter selection method and has been reported to be successful in many applications. The ranking

method comprises two steps: feature ranking and selection of the feature that has the highest ranking [45].

Based on the concepts that are described above, we present a new filter ranking feature algorithm that has the benefits of filter approaches and realizes high performance. We propose a new ranking feature that is based on a statistical description by using the PDF. Statistics offers powerful specialized procedures for testing the significance of differences between means [46]. The primary reason for the application of feature ranking in this study is to rank the features that influence the recognition process. In the current study, we improved the feature ranking process by employing the PDF as described by Algorithm 2.

Algorithm 2 Feature Selection

Step 1: Input feature matrix [i, j]:

- For i = 1, i < length of matrix, i++
- For j = 1, j < number of features, j++
- Read X, X = $\{x_{1.1}, x_{2.1}, \ldots\ldots\ldots x_{i,\ 1}, x_{i,\ j}\}$($x_{i,\ j}$ = feature value per cell)

Step 2: Determine the PDF:

- For each j, compute the standard deviation PDF as:

$$s = \sqrt{\sum [x^2 * P(x)] - \mu^2} \tag{2}$$

where:

s : the standard deviation, which is a value that expresses the extent by which the elements of a series vary from the mean;

$P(x)$: the probability, $P(x) = \frac{nx}{nX}$;

μ : the mean, $\mu = \sum [x.P(x)]$.

Each feature column j returns one value of the standard deviation PDF;

Step 3: Rank the standard deviation PDF values in descending order (from high to low);

Step 4: Rank the feature matrix index based on its standard deviation PDF ranking;

Step 5: Return the ranking feature matrix [i, j];

Step 6: Select the features that are highly ranked.

Step 7: Go to the recognition step.

E. RECOGNITION

PNN is an artificial neural network algorithm. It is extensively used in classification problems and in pattern recognition. PNN was developed by Donald Specht [48]. He proved that backpropagation (BP) must run for 3 weeks to realize an accuracy 82%, while PNN requires 0.7 sec to realize the same accuracy; hence, PNN is 200,000 times faster than BP. Furthermore, PNN training is straightforward and instantaneous, and it can be used in real time because as soon as one pattern that represents each category has been observed, the network can begin to generalize to new patterns. Therefore, this study adopts PNN as a recognition algorithm due to its simplicity and accurate classification results in minimum time.

In the basic PNN, the probability density function (pdf) is estimated using the complete training set for each class. The learning algorithm that is used to train PNN will be supervised, and the output class will be learned first. In a supervised learning classification technique, a new input vector X*new* should be classified into one of the classes that has the largest posterior probability. When no a priori information is known about the classes, Bayesian theory is used. In addition, the PNN algorithm uses the Parzen window to estimate the pdf of class Ci by averaging the multivariate normal Gaussian kernels that are centered at each training sample. The PNN architecture includes four layers: In the input layer, the testing symbols are specified (query class). In the pattern layer, training patterns are loaded. The summation layer calculates the sum of the pdfs.

The output layer (decision layer) identifies the class label based by comparing all the results from the summation layer and selecting the result that correspond to the largest sum value [47].

The PNN algorithm consists of three steps: kernel calculation, class conditional probability (pdf) and choosing the maximum class conditionally.

Here, the PNN collaborates with the feature selection step; hence, after ranking the features, we select various numbers of features and feed them into the PNN to classify the palmprint. We denote the palmprint subject by a class; each class Ci has a group that consists of eight subset classes, Ci, j, and each subset per class has a feature vector (X). Algorithm 3 and Figure 4 describe the recognition process. In addition, the PNN is enhanced by using the epoch concept and random shuffling. An epoch represents one iteration over the entire dataset, and various numbers of epochs are used until high accuracy is realized. At each epoch, the palmprint sub classes are selected randomly for both the training and testing sets based on random shuffling.

IV. EXPERIMENT AND RESULTS

This section presents the experimental results and performance evaluation of the proposed method. For validation, a confusion matrix has been used, and the equal error rate (EER), accuracy rate, and receiver operating characteristic (ROC) curve were used as metrics in the assessment standard. The proposed scheme was tested by using high-resolution palmprints from THUPALMLAB. We evaluated the proposed scheme by dividing the database into a training set and a testing set according to ratios 50%:50% and 80%:20%. The database will be described in subsection A. Subsection B summarizes the palmprint ROI extraction method; the creation of the feature matrix will be explained in subsection C. In subsection D, the ranking of the feature matrix based on its PDF will be discussed. Finally, the proposed scheme will be evaluated and the results will be compared in more detail in subsection E. The visual studio C#

Algorithm 3 Feature Recognition

$Ts = \{Ci\}$, $Ci = [X_{Ci,j}]$, Ts: feature set

$Ts = [X_{Ci,j}]$, $[X_{Ci,j}]$: the feature ranking matrix

Step 1: Select features:

Input data X_{new};

- Extract feature X_{new};
- Rank features of X_{new} based on the feature ranking matrix index;
- Select k features.

Step 2: PNN computation

- Input the selected features
- Calculate the Gaussian kernel (w_{ij}) of $X_{Ci,j}$ [47], [48]

$$w_{ij} = \frac{1}{(2\pi)^{\frac{d}{2}}\,\sigma^d} \times exp(-\frac{\left(X_{new}-X_{Ci,j}\right)^T . \left(X_{new}-X_{Ci,j}\right)}{2\sigma^2} \tag{3}$$

where $0 \leq \sigma \leq 1$, and the variation of σ *does* not affect the estimate of the pdf

- Calculate the class conditional probability based on the Parzen window method [49] of Ci:

$$\mathrm{P}(X_{new}|C_i) = P_{i=}\frac{1}{|C_i, j|}\sum_{j=1}^{|C_{i,j}|} w_{ij} \tag{4}$$

- Select the class with the highest pdf as the class of the new input data [X_{new}] based on Bayesian theory [48].

$class\,(X_{new}) = \{P\,(Ci)\}$

(Microsoft Visual Studio 2013) is used to implement the experiments.

A. THUPALMLAB DATABASE

THUPALMLAB is the only publicly available high-resolution database [50]. It consists of 1,280 palmprints (left and right palmprints per person with 8 samples per palmprint) from 80 subjects, which were acquired by using a palmprint scanner of Hisign. The database images are of size 2040 × 2040 pixels and 500-ppi resolution. We will use 800 images from the first 50 palmprints (left and right) (50 × 2 × 8). A sample of the palmprint images in the THUPALMLAB database is shown in Figure 5.

B. PALMPRINT ROI EXTRACTION

Based on the method that was introduced in [37] and described in the preprocessing section, the palmprint ROIs have been extracted. Figure 6 summarizes the steps for extracting the palmprint ROIs.

C. CREATING THE FEATURE MATRIX

To create the feature matrix [i, j], texture features are extracted from the ROI palmprint by applying the proposed

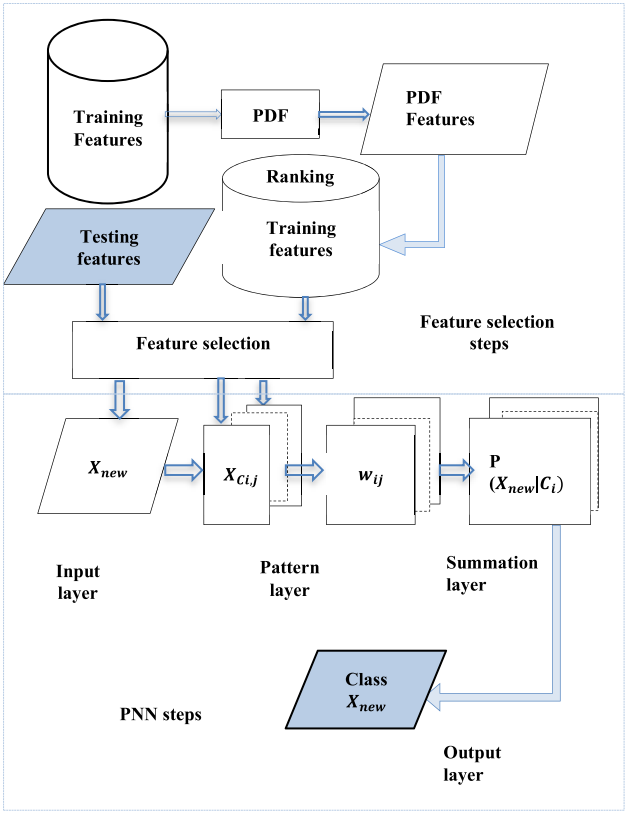

FIGURE 4. Recognition model.

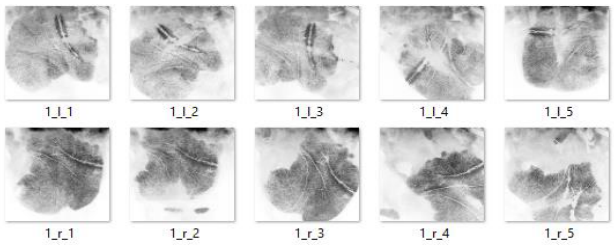

FIGURE 5. A sample of palmprint images in THUPALMLAB database.

Algorithm 1. These features have a wide range of values and most features are overlapping; thus, a suitable standardization rule should be considered [51]. Figure 7 illustrates the original and standardized features.

After standardization of the features values and the application of the concatenation rule, the feature matrix [i, j] is of dimensions [(4 × 13), (50 × 2 × 8)]. These features represent input palmprint characteristics.

D. SELECTING FEATURES

To select features, we apply the proposed Algorithm 2 to the feature matrix [i, j]. First, we determine the PDF for these features. Second, we rank feature matrix [i, j] in descending order based on the PDF values, where the features with the largest PDF values have a high-ranking index.

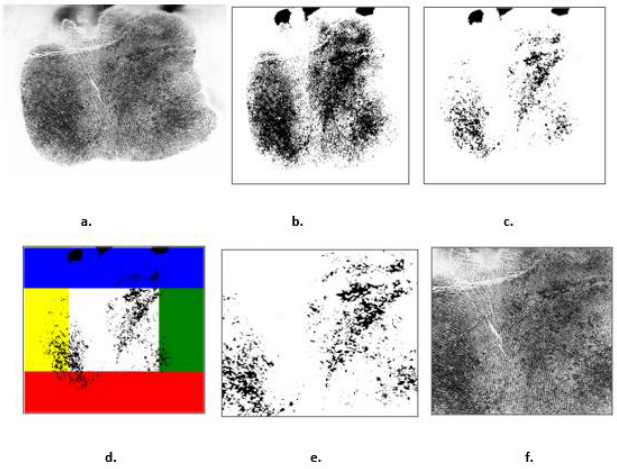

FIGURE 6. Palmprint ROI extraction steps a. Original palmprint b. Binerzation palmprint c. Dilated palmprint d. Divided palmprint four regions e. Binary ROI palmprint f. Gray ROI palmprint.

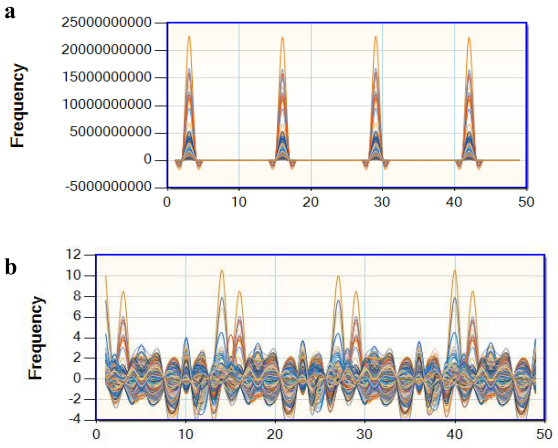

FIGURE 7. Features a. Original, and b. Standardization.

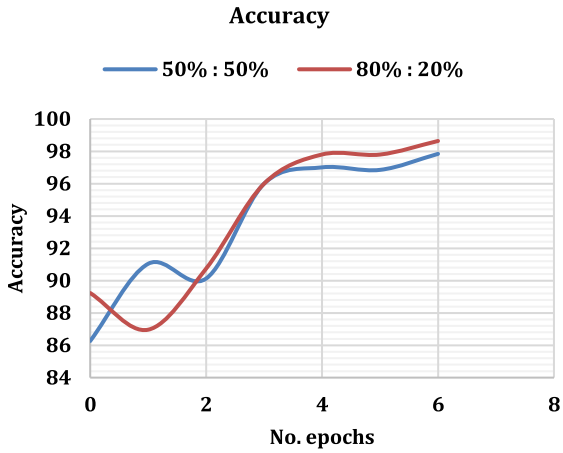

FIGURE 8. Performance of the accuracy rate based multiple epochs.

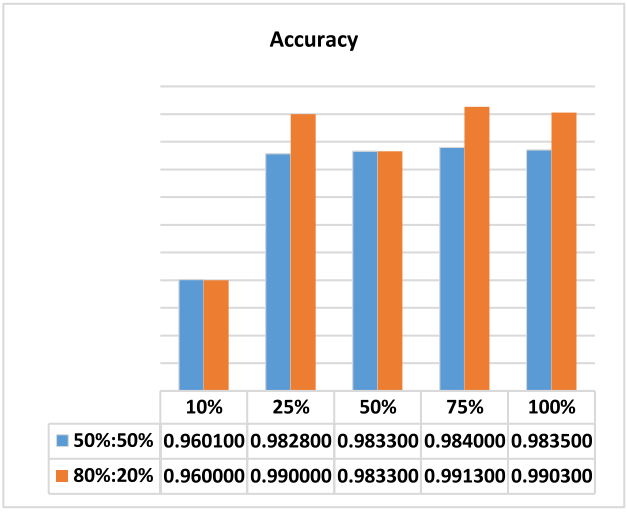

	10%	25%	50%	75%	100%
50%:50%	0.960100	0.982800	0.983300	0.984000	0.983500
80%:20%	0.960000	0.990000	0.983300	0.991300	0.990300

FIGURE 9. Accuracy rate for ratios 50%:50%, and 80%:20% data division.

Finally, we select ranked features by specifying the number of features.

To evaluate the significance of the effect of these ranked features on the recognition performance, 10%, 25%, 50%, 75%, and 100% of the features have been selected for the experiments.

E. RECOGNITION SCHEME EVALUATION AND COMPARISON

After the completion of all the steps, the multimodal scheme performance is evaluated by applying the proposed Algorithm 3. First, Figure 8 shows the effects of increasing the number of epochs on the recognition accuracy rate for ratios 50%:50% and 80%:20%.

According to Figure 8, the performance increases as the number of epochs increases. Hence, we consider 7 epochs in the final implementation (according to our experiment, after 7 epochs, the rate is fixed).

Afterword, the performance of the proposed scheme is evaluated using various numbers of features, as shown in Figures 9 and 10.

According to Figures 9 and 10, the ranking feature has a more positive effect on recognition, and we can realize high performance by using a subset of the features. For the ratio of 50%:50%, the accuracy rate is 0.9601 for 10% of the features, compared to 0.9835 for 100% of the features, which is a difference of only approximately 0.02. In addition, the difference among the accuracy rates for 25%, 50%, and 75% of the features is approximately 0.001. The EER for 10% of the features is 0.0399, while for 25%, 50%, 75%, and 100% of the features the values are 0.0172, 0.0167, 0.0160, and 0.0165, respectively, which are very close.

In addition, for the ratio 80%:20%, the accuracy rate is between 0.9600-0.9903 for 10% and 100% of the features, respectively, which represents a difference of 0.03, and an approximate difference of 0.008 is observed among the remaining features (25%, 50%, and 75%). For EER,

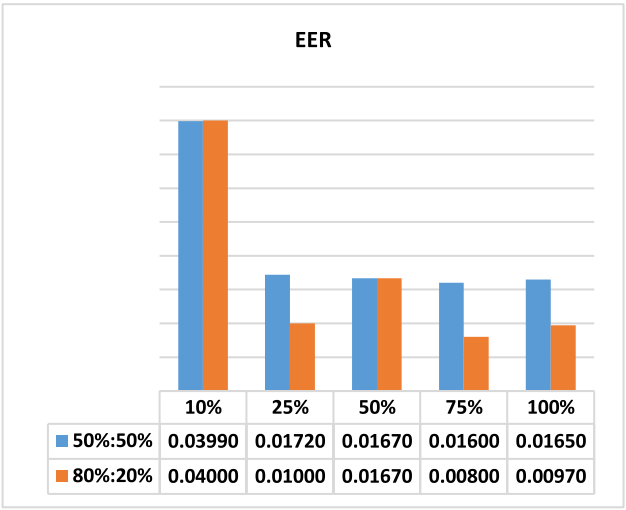

FIGURE 10. EER for ratios 50%:50%, and 80%:20% data division.

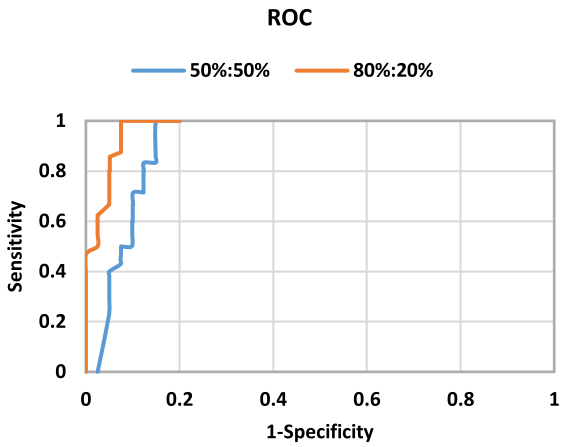

FIGURE 11. ROC curves for ratios 50%:50%, and 80%:20% data division.

TABLE 2. Comparison of previous studies with the proposed scheme.

Reference	Algorithm	EER%	Model
[33] Manual regions	SMC	14.2	Unimodal
[33] Automatic regions	SMC	11.46	Unimodal
[1]	PP-KMDER	13.97	Unimodal
[29]	PP-KMDER. + PP-RIDER	13.97	Unimodal
Proposed 50%:50%	GLCM + PNN	1.6	Multimodal
Proposed 80%:20%	GLCM + PNN	0.88	Multimodal

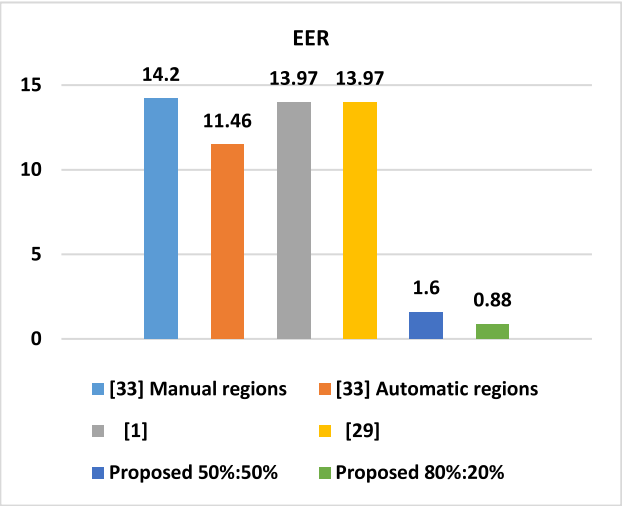

FIGURE 12. EER of previous studies with the proposed scheme.

we obtain 0.040-0.0097 for 10% and 100%, respectively, of the features, and the difference among the rates for the remaining features (25%, 50%, and 75%) is approximately 0.009.

The best results for the ratio 50%:50% are 0.9840 and 0.016 for the accuracy rate and EER, respectively, with 75% of the features, and the best results for the ratio 80%:20% are 0.9913 and 0.008 for the accuracy and EER, respectively, with 75% of the features. The results are presented as ROC curves for both 50%:50% and 80%:20% with 75% of the features in Figure 11, which demonstrate high recognition accuracy.

The proposed scheme has been evaluated, and we demonstrated that highly satisfactory recognition results are obtained in a short time of approximately 0.218 sec. In addition, the results clearly demonstrate that the feature selection method performs more effectively and improves the recognition step.

The results of this study for high-resolution palmprints are compared with those that have been reported in the literature. However, this comparison has several limitations, as no study is similar to ours. In these studies, different criteria and databases were used, thereby rendering direct comparisons difficult.

However, our new recognition process was evaluated by comparing our results with those of the previous studies that are most similar to ours, which utilized the THUPALMLAB database. These studies were introduced in Section 2. Table 2 and Figure 12 summarize this comparison.

The performance evaluation results of our proposed method demonstrate that the use of left and right palmprints compared to a single palmprint is more effective in person recognition using high-resolution palmprints.

V. CONCLUSION

This study proposed a multimodal scheme in which left and right palmprints are combined, which realizes satisfactory performance for high-resolution images. The proposed scheme, which is based on texture features for effective texture discrimination, ranks features by using a novel method in which a PDF is employed and the PNN is used as a faster classifier. Therefore, this scheme is considered state of the art

in biometric systems. The current study demonstrates that the multimodal palmprint is an improvement over the traditional palmprint in forensic applications. Since humans have similar palmprint traits between their left and right hands, a lack of features from one hand can be compensated by features from the other. These similarities can facilitate the realization of a higher result rate than those of conventional methods.

REFERENCES

[1] L. Carreira, P. L. Correia, and L. D. Soares, "On high resolution palmprint matching," in *Proc. 2nd Int. Workshop Biometrics Forensics*, Mar. 2014, pp. 1–6.
[2] Z. Dandan, X. Pan, X. Luo, and X. Gao, "Palmprint recognition based on deep learning," in *Proc. 6th Int. Conf. Wireless, Mobile Multi-Media (ICWMMN)*, Nov. 2015, pp. 214–216.
[3] S. Minaee and Y. Wang, "Palmprint recognition using deep scattering convolutional network," 2016, *arXiv:1603.09027*. [Online]. Available: http://arxiv.org/abs/1603.09027
[4] L. Leng and A. B. J. Teoh, "Alignment-free row-co-occurrence cancelable palmprint fuzzy vault," *Pattern Recognit.*, vol. 48, no. 7, pp. 2290–2303, Jul. 2015.
[5] D. Hong, W. Liu, X. Wu, Z. Pan, and J. Su, "Robust palmprint recognition based on the fast variation Vese–Osher model," *Neurocomputing*, vol. 174, pp. 999–1012, Jan. 2016.
[6] E. Sujatha and A. Chilambuchelvan, "Multimodal biometric authentication algorithm using iris, palm print, face and signature with encoded DWT," *Wireless Pers. Commun.*, vol. 99, no. 1, pp. 23–34, Mar. 2018.
[7] Y. Jain and M. Juneja, "A novel approach for multimodal biometric system using Iris and palmprint," in *Progress in Advanced Computing and Intelligent Engineering*. Singapore: Springer, 2018, pp. 79–88.
[8] T. Z. Lee and D. B. L. Bong, "Face and palmprint multimodal biometric system based on bit-plane decomposition approach," in *Proc. IEEE Int. Conf. Consum. Electron.-Taiwan (ICCE-TW)*, May 2016, pp. 1–2.
[9] M. M. Jazzar and G. Muhammad, "Feature selection based Verification/Identification system using fingerprints and palm print," *Arabian J. Sci. Eng.*, vol. 38, no. 4, pp. 849–857, Apr. 2013.
[10] M. Bellaaj, R. Boukhris, A. Damak, and D. Sellami, "Possibilistic modeling palmprint and fingerprint based multimodal biometric recognition system," in *Proc. Int. Image Process., Appl. Syst. (IPAS)*, Nov. 2016, pp. 1–8.
[11] H. Naderi, B. H. Soleimani, and S. Matwin, "Manifold learning of overcomplete feature spaces in a multimodal biometric recognition system of iris and palmprint," in *Proc. 14th Conf. Comput. Robot Vis. (CRV)*, May 2017, pp. 191–196.
[12] N. Hezil and A. Boukrouche, "Multimodal biometric recognition using human ear and palmprint," *IET Biometrics*, vol. 6, no. 5, pp. 351–359, Sep. 2017.
[13] D. Samai, A. Meraoumia, S. Chitroub, N. Doghmane, and A. Taleb-Ahmed, "Multimodal biometric system based on palmprint using progressive image compression," in *Proc. Int. Conf. Inf. Technol. Org. Develop. (ITOD)*, Mar. 2016, pp. 1–4.
[14] A. Lumini and L. Nanni, "Overview of the combination of biometric matchers," *Inf. Fusion*, vol. 33, pp. 71–85, Jan. 2017.
[15] Y. Xu, L. Fei, and D. Zhang, "Combining left and right palmprint images for more accurate personal identification," *IEEE Trans. Image Process.*, vol. 24, no. 2, pp. 549–559, Feb. 2015.
[16] L. Leng, M. Li, C. Kim, and X. Bi, "Dual-source discrimination power analysis for multi-instance contactless palmprint recognition," *Multimedia Tools Appl.*, vol. 76, no. 1, pp. 333–354, Jan. 2017.
[17] L. Fei, G. Lu, W. Jia, S. Teng, and D. Zhang, "Feature extraction methods for palmprint recognition: A survey and evaluation," *IEEE Trans. Syst., Man, Cybern. Syst.*, vol. 49, no. 2, pp. 346–363, Feb. 2019.
[18] S. Lin and Y. Tai, "A combination recognition method of palmprint and palm vein based on gray surface matching," in *Proc. 8th Int. Congr. Image Signal Process. (CISP)*, Oct. 2015, pp. 567–571.
[19] A. Kong, D. Zhang, and M. Kamel, "A survey of palmprint recognition," *Pattern Recognit.*, vol. 42, no. 7, pp. 1408–1418, Jul. 2009.
[20] D. Zhang, W. Zuo, and F. Yue, "A comparative study of palmprint recognition algorithms," *ACM Comput. Surveys*, vol. 44, no. 1, pp. 1–37, Jan. 2012.
[21] I. Beheshti and H. Demirel, "Probability distribution function-based classification of structural MRI for the detection of Alzheimer's disease" *Comput. Biol. Med.*, vol. 64, pp. 208–216, Sep. 2015.
[22] H. Demirel and G. Anbarjafari, "Pose invariant face recognition using probability distribution functions in different color channels," *IEEE Signal Process. Lett.*, vol. 15, pp. 537–540, 2008.
[23] M. N. Akram and S. Lotfifard, "Modeling and health monitoring of DC side of photovoltaic array," *IEEE Trans. Sustain. Energy*, vol. 6, no. 4, pp. 1245–1253, Oct. 2015.
[24] X. Li, S. Zhang, S. Li, and J. Chen, "An improved method of speech recognition based on probabilistic neural network ensembles," in *Proc. 11th Int. Conf. Natural Comput. (ICNC)*, Aug. 2015, pp. 650–654.
[25] A. K. Jain and J. Feng, "Latent palmprint matching," *IEEE Trans. Pattern Anal. Mach. Intell.*, vol. 31, no. 6, pp. 1032–1047, Jun. 2009.
[26] S. Singh, M. Ramalho, P. L. Correia, and L. D. Soares, "PP-RIDER: A rotation-invariant degraded partial palmprint recognition technique," in *Proc. 20th Eur. Signal Process. Conf. (EUSIPCO)*, Aug. 2012, pp. 1499–1503.
[27] S. Singh, P. L. Correia, and L. D. Soares, "Improved rotation-invariant degraded partial palmprint recognition technique," in *Proc. Int. Workshop Biometrics Forensics (IWBF)*, Apr. 2013, pp. 1–4.
[28] F. Brusius, U. Schwanecke, and P. Barth, "Blind image deconvolution of linear motion blur," in *Proc. Int. Conf. Comput. Vis., Imag. Comput. Graph.* Berlin, Germany: Springer, 2011, pp. 105–119.
[29] L. Carreira, P. L. Correia, L. D. Soares, and S. Singh, "Personal identification from degraded and incomplete high resolution palmprints," *IET Biometrics*, vol. 4, no. 2, pp. 53–61, Jun. 2015.
[30] R. Wang, D. Ramos, and J. Fierrez, "Improving radial triangulation-based forensic palmprint recognition according to point pattern comparison by relaxation," in *Proc. 5th IAPR Int. Conf. Biometrics (ICB)*, Mar. 2012, pp. 427–432.
[31] R. Wang, D. Ramos, J. Fierrez, and R. P. Krish, "Automatic region segmentation for high-resolution palmprint recognition: Towards forensic scenarios," in *Proc. 47th Int. Carnahan Conf. Secur. Technol. (ICCST)*, Oct. 2013, pp. 1–6.
[32] R. Wang, D. Ramos, J. Fierrez, and R. P. Krish, "Towards regional fusion for high-resolution palmprint recognition," in *Proc. 26th Conf. Graph., Patterns Images*, Aug. 2013, pp. 357–361.
[33] R. Wang, D. Ramos, J. Fierrez, R. Veldhuis, H. Xu, and L. Spreeuwers, "Regional fusion for high-resolution palmprint recognition using spectral minutiae representation," *IET Biometrics*, vol. 3, no. 2, pp. 94–100, Jun. 2014.
[34] M. Laadjel, F. Kurugollu, A. Bouridane, and S. Boussakta, "Degraded partial palmprint recognition for forensic investigations," in *Proc. 16th IEEE Int. Conf. Image Process. (ICIP)*, Nov. 2009, pp. 1513–1516.
[35] J. Dai and J. Zhou, "Multifeature-based high-resolution palmprint recognition," *IEEE Trans. Pattern Anal. Mach. Intell.*, vol. 33, no. 5, pp. 945–957, May 2011.
[36] T. Faisal, K. Benatchba, and M. Koudil, "Matching similarity scores for a minutiae-based palmprint recognition," in *Proc. 45th Annu. Conf. IEEE Ind. Electron. Soc. (IECON)*, vol. 1, Oct. 2019, pp. 132–137.
[37] I. S. Hussein, S. B. Sahibuddin, M. J. Nordin, and N. N. Amir, "The extract region of interest in high-resolution palmprint using 2D image histogram entropy function," *J. Comput. Sci.*, vol. 15, no. 5, pp. 635–647, May 2019.
[38] F. B. Legesse, A. Medyukhina, S. Heuke, and J. Popp, "Texture analysis and classification in coherent anti-Stokes Raman scattering (CARS) microscopy images for automated detection of skin cancer," *Comput. Med. Imag. Graph.*, vol. 43, pp. 36–43, Jul. 2015.
[39] L. Nanni, S. Brahnam, S. Ghidoni, E. Menegatti, and T. Barrier, "Different approaches for extracting information from the co-occurrence matrix," *PLoS ONE*, vol. 8, no. 12, 2013, Art. no. e83554.
[40] R. M. Haralick, K. Shanmugam, and I. Dinstein, "Textural features for image classification," *IEEE Trans. Syst., Man, Cybern.*, vol. SMC-3, no. 6, pp. 610–621, Nov. 1973.
[41] N. Charfi, H. Trichili, A. M. Alimi, and B. Solaiman, "Bimodal biometric system for hand shape and palmprint recognition based on SIFT sparse representation," *Multimedia Tools Appl.*, vol. 76, no. 20, pp. 20457–20482, Oct. 2017.
[42] R. Mokni, H. Drira, and M. Kherallah, "Fusing multi-techniques based on LDA-CCA and their application in palmprint identification system," in *Proc. IEEE/ACS 14th Int. Conf. Comput. Syst. Appl. (AICCSA)*, Oct. 2017, pp. 350–357.

[43] D. Hong, W. Liu, J. Su, Z. Pan, and G. Wang, "A novel hierarchical approach for multispectral palmprint recognition," *Neurocomputing*, vol. 151, pp. 511–521, Mar. 2015.
[44] G. S. Srivastava, "Accurate human recognition by score-level and feature-level fusion using palm–phalanges print," *Arabian J. Sci. Eng.*, vol. 43, no. 2, pp. 543–554, 2018.
[45] T. A. Alhaj, M. M. Siraj, A. Zainal, H. T. Elshoush, and F. Elhaj, "Feature selection using information gain for improved structural-based alert correlation," *PLoS ONE*, vol. 11, no. 11, 2016, Art. no. e0166017.
[46] J. Yang, Y. Liu, Z. Liu, X. Zhu, and X. Zhang, "A new feature selection algorithm based on binomial hypothesis testing for spam filtering," *Knowl.-Based Syst.*, vol. 24, no. 6, pp. 904–914, Aug. 2011.
[47] I. Klebanov, "Axiomatic approach to variable kernel density estimation," 2018, *arXiv:1805.01729*. [Online]. Available: http://arxiv.org/abs/1805.01729
[48] M. Ahmadlou and H. Adeli, "Enhanced probabilistic neural network with local decision circles: A robust classifier," *Integr. Comput.-Aided Eng.*, vol. 17, no. 3, pp. 197–210, Jul. 2010.
[49] T. Cacoullos, "Estimation of a multivariate density," *Ann. Inst. Statist. Math.*, vol. 18, no. 1, pp. 179–189, Dec. 1966.
[50] *THUPALMLAB Palmprint Database*. Tsinghua University. [Online]. Available: http://ivg.au.tsinghua.edu.cn/index.php?n=Data.Tsinghua500ppi
[51] A. Jain, K. Nandakumar, and A. Ross, "Score normalization in multimodal biometric systems," *Pattern Recognit.*, vol. 38, no. 12, pp. 2270–2285, Dec. 2005.

INASS SHAHADHA HUSSEIN is currently pursuing the Ph.D. degree with the Faculty Razak of Technology and Informatics, UTM, Kuala Lumpur, Malaysia. She is currently a Lecturer with the Baquba Technical Institute, Middle Technical University, Baquba, Iraq. Her research interests include machine learning, biometric systems, and pattern recognition.

SHAMSUL BIN SAHIBUDDIN received the B.S. degree in computer science from National Chung Western Michigan University, Kalamazoo, MI, USA, in 1986, the M.S. degree in computer science from Central Michigan University, Mount Pleasant, MI, in 1988, and the Ph.D. degree in computer science from Aston University, Birmingham, U.K., in 1998. He is currently a Professor with the Faculty Razak of Technology and Informatics, UTM, Kuala Lumpur, Malaysia. His current research interests include computer science and software engineering.

MD JAN NORDIN (Member, IEEE) received the B.S. and M.S. degrees in computer science from Ohio University, Athens, OH, USA, in 1982 and 1985, respectively, and the Ph.D. degree in engineering information technology from Sheffield Hallam University, South Yorkshire, U.K., in 1995. He is currently an Associate Professor with the Center for Artificial Intelligence Technology, Universiti Kebangsaan Malaysia, Malaysia. His current research interests include pattern recognition, computer vision, intelligent systems, and image reconstruction.

NILAM NUR BINTI AMIR SJARIF received the B.Sc. degree in computer science (software engineering), in 2010, and the Ph.D. degree in computer science from the Universiti Teknologi Malaysia, Kuala Lumpur, in 2015, with a focus on human action recognition with the geometrical feature representation for video surveillance. She is currently a Senior Lecturer with the Department of Advanced Infomatics, Faculty Razak of Technology and Informatics, Universiti Teknologi Malaysia. Her current research interests include image and video processing, pattern recognition, machine learning, deep learning, watermarking, and big data analytics.